Influence of sperm impact angle on successful fertilization through mZP oscillatory spherical net model

Andjelka Hedrih [a,*], Mihailo Lazarevic [b], Ana Mitrovic-Jovanovic [c]

[a] *Department for Bio-medical Science, State University of Novi Pazar, Novi Pazar, Vuka Karadzica bb, 36 300 Novi Pazar, Serbia*
[b] *Faculty of Mechanical Engineering, University of Belgrade, Kraljice Marije 16, 11 120 Belgrade, Serbia*
[c] *School of Medicine, University of Belgrade, Dr Subotica 8, 11 000 Belgrade, Serbia*

A B S T R A C T

According to the available literature, penetrating sperm creates an oblique path trough Zona pellucida (ZP) – the most outer surface of oocytes. Considering fertilization process as an oscillatory phenomenon, the influence of sperm impact angle relative to the oscillatory behavior of mouse ZP is described by using the discrete continuum mechanical model in the form of a spherical net model.

A parametric frequency analysis of oscillatory behavior of knot material particles in the mouse ZP (mZP) spherical net model is conducted by using generalized Lussajous curves. The influence of impact angles of sperm cells on the corresponding knot mass particles' resultant trajectory is discussed. Favorable sperm impact angles for successful fertilization are identified.

© 2015 Elsevier Ltd. All rights reserved.

1. Introduction

Studying the sperm–oocyte interaction is important for understanding the process of fertilization. The precise molecular mechanism of mammalian fertilization is still not known, but from biochemical point of view it is considered that fertilization passes through several phases: recognition and specific receptor binding of sperm cell to ZP, acrozome reaction, penetration of sperm head trough zona pelucida, and cortical reaction [1]. In the process of fertilization both oocyte and spermatozoa pass through structural and biochemical changes [2]. "During the activation of the sperm cell (i.e. capacitation) in the female genital tract, dramatic reorganizations take place in the sperm plasma membrane in order to achieve the ability to fertilize the oocyte [3]." Certain amount of spermatozoa that undergo acrosome reaction at the time of insemination is required for fertilization to be successful. By using images of boar spermatozoa obtained with an optical phase-contrast microscope and learning vector quantization, Alegre et al. [4] automatically classify individual sperm cells as acrosome-intact or acrosome-damaged with an overall test error of 6.8%.

Clark [5] gave an alternative theory for successful sperm–ZP binding events and post-fertilization inhibition of sperm binding.

According to this theory, content of the cortical granules causes modification of ZP2 that leads to modification of ZP3 that lacks sperm receptor and acrosome-inducing activity. Modified ZP2 and ZP3 are unsuitable for binding either acrosome reacted or acrosome intact sperm cells. The precise mechanism of how spermatozoa pass through *ZP* is still unclear. This process should have particular timing as ZP dynamically changes its mechanical properties during the processes of oogenesis, fertilization, and pre-implantation development [6–12]. Ultrastructural analysis of mammal ZP by using transmission electronic microscopy (TEM) showed that the spermatozoid penetrated ZP by an oblique path [13,14], but the specific angle is still not known. "Binding of the sperm head by its flat surface could initiate the oblique angle of its subsequent penetration through the eutherian zona. The tangential trajectory of that path ensures that it then closes as the zona stretches and thins during expansion of the blastocyst, so preventing the development of a hole(s)" [14]. Neither *in vivo* nor *in vitro* conditions of fertilization are always successful. Bayesian classifiers can be used to predict suitability of an embryo to succeed implantation [15]. Corani et al. [16] made a network model for predicting pregnancy after *in vitro* fertilization (IVF). The authors compare the proposed model with classification algorithms in the analysis of a data set containing IVF cycles performed at reproductive institute. There are several biomechanical models describing sperm–oocyte interaction from the biomechanical point of view [17–19]. Using contact mechanics based modeling Gefen [17] modeled relationship between sperm velocity and pressures applied to the ZP during early sperm–oocyte

* Correspondence to: Trg Ucitelj Tase 3/9, 18 000 Nis, Serbia.
Tel.: +381 64 801 33 20; fax: +381 18 42 41 663.
E-mail addresses: handjelka@hm.co.rs, handjelka@gmail.com (A. Hedrih).

penetration. The analysis showed that sperm velocity had higher impact on pressure generated at the ZP surface than the sperm head density. Modeling of Kozlovsky and Gefen [18] predicted that during the early stage of penetration into ZP, biochemical binding forces acting on spermatozoa, which have effective velocities, are less than the mechanically generated propulsive forces.

According to the modeling of sperm–oocyte interaction in [19], the hyperactivation of the spermatozoon and the sharpness of the spermatozoon head are all important factors that govern successful sperm penetration into ZP. Their modal analysis revealed that ZP hardening process as well as ZP thickness had a negligible effect on the maximum contact pressures, and the maximum penetration of the head of spermatozoon. The biomechanical model presented in [20,21] suggests that, in most cases interaction between spermatozoa and ovum prior to sperm penetration, result in rotation of the egg as a result of the previously unstable state.

According to our knowledge, there are no experimental data about specific angle of sperm–ZP interaction that leads to successful fertilization, nor data on whether this specific value of this angle depends on acrosome reaction. It is possible that size of the exact angle varies between species of mammals i.e. varies with the composition of ZP and shape and size of spermatozoa head which is species-specific.

Angle at which a spermatozoid influences ZP of the oocyte is important for understanding the process of mammalian fertilization and mechanical properties of ZP.

Practical value of knowing this angle is in the application of this knowledge in intracytoplasmatic sperm injection (ICSI) artificial fertilization technique. Knowing angles under which spermatozoa influence ZP and by using this knowledge in this technique could possibly increase its efficiency and have multiple benefits. In ICSI technique, during contact of micro-injection needle and ZP surface forced oscillations of ZP appear. From the point of view of theory of oscillations, each cell, each molecule, will exhibit oscillatory movement. Self-oscillations are existent in the basal state. Forced oscillations appear upon action of a force. The oscillatory behavior of embryo in micro-injection technique which is used for measurement of elastic properties of ZP has been analyzed in [21] by using the finite element method. In addition, the micro-tactile sensors used for measurement of elastic properties of ZP in [7] are operating on the basis of piezoelectric effect, i.e. they measure difference in the resonance frequency of the material in contact with the sensor which confirms that oscillatory behavior of ZP exists and can be measured.

In this paper we extend the analysis presented in [22,23,24], by discussing a model that in comparison with the models used in the previously considered analyses, contains additional variables (sperm impact angle and sperm velocity).

1.1. The basic idea of sperm–oocyte oscillatory interaction

The basic concept is that oocyte is an oscillatory structure which changes its oscillatory state as it changes its maturity status. The most of the outer surface which resembles a 3D mash (on SEM) changes its mechanical properties during different maturation states [6–12] as well as its oscillatory state [25]. The structure can oscillate in a free or in a forced regime. These oscillations involve multiple frequencies. In a forced oscillatory regime, a resonance could occur. In a state of resonance, as amplitudes of oscillations enlarge, break of some "weak spot" in the ZP is possible. This week spot could be the spot for initial penetration of "the chosen sperm". According to this oscillatory theory of fertilization, the "chosen sperm" will be the sperm who oscillates long enough at one of the ZP eigen frequencies. Impact of the other spermatozoa on the ZP surface could contribute to this resonant state of ZP.

In order to describe the oscillatory behavior of ZP structure and, inspired by the Wassermans' model of mouse ZP (mZP) [26], 3D structural changes of ZP in atomic force microscope (AFM) [27], and scanning electron microscope (SEM) analysis [28], we create an oscillatory spherical net model [22–24,29]. The molar ratio and masses of mZP glycoproteins were included in the model. Material particles in the ZP oscillatory spherical net model correspond to the ZP glycoproteins (see Fig. 1A and B). Knot material particles (molecules) correspond to the ZP1 glycoproteins. Chemical structure of ZP is similar in mice, rats, pigs, and humans. In mice, ZP consists of 3 sulphated glycoproteins: ZP1, ZP2, and ZP3. The ratio of ZP2:ZP3 in mice is close to 1:1, whereas ZP1: (ZP2–ZP3) is 1:5. ZP2 and ZP3 are of fibril structure. They are interchangeably connected making fibril structures that are cross-linked with ZP1. Relative molecular masses of the three proteins in mouse are: (MrZP1): 200 000 Da, (MrZP2): 120 000 Da, and (MrZP3): 83 000 Da [26].

Parametric frequency analysis of oscillatory behavior of knot molecules in mZP spherical net model was done by using generalized Lussajous curves. The influence of impact angles of sperm cells on the corresponding knot mass molecules resultant trajectory is discussed.

By using certain combinations of sperm cell impact angles, it is possible to achieve different ratios of component amplitudes of 11 harmonics in the equations for displacement of each knot
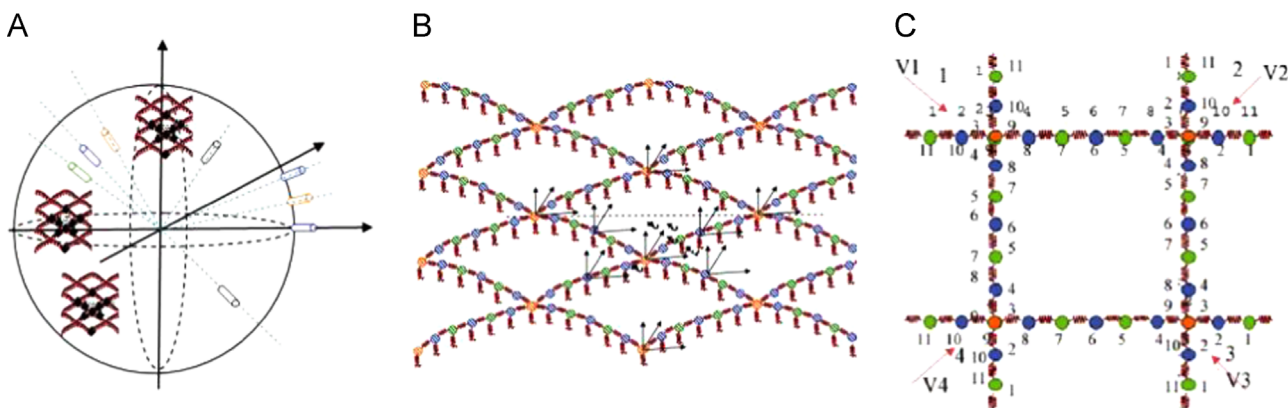
Fig. 1. (A) Model of ZP spherical surface that shows radial direction of axis of constructive elements of the model – ZP proteins. (B) Part of the ZP network on a part of the sphere (oocyte). Orange (ZP1), blue (ZP2) and green (ZP3) represents molecules of ZP proteins. Chains of spherical net are identical in circular and meridian direction. Axes show directions of movements of molecules of ZP proteins. Each ZP protein is connected to the sphere with elastic springs that can oscillate in radial direction. (C) Segment of spherical surface net model of mZP; V1–V4 are sperm cells with effective velocities. Red arrows denote sperm cell impact on a knot molecule. (For interpretation of the references to color in this figure legend, the reader is referred to the web version of this article.)

molecule in the radial, meridian, and circular directions. For the case of free oscillations, knot molecules oscillate in three directions: in the meridian and circular directions (with 11 frequencies in each direction) and in the radial direction with a single-frequency. In the case of forced oscillations, when a single-frequency external excitation is applied in the radial direction to the knot molecule, it has two-frequency component displacements.

Stacking the orthogonal asynchronous oscillations involving 11 equally probable frequencies of different amplitudes and phases, we could obtain different resultant trajectories of each knot molecule. The resultant trajectories of each knot molecule lie in the plane tangential to the sphere surface net.

According to the form of generalized Lissajous curves, dynamical state of knot molecules could be in the form of full synchronization or asyinchronism, look like synchronization or asyinchronism or look like chaotic or stochastic like states. If all considered knot molecules oscillate synchronously in the tangential plane, the outcome of impact of the sperm cell at ZP could be predictable. In the case of synchronization of the resultant motion of knot molecules, new spermatozoa can pass through ZP net. We consider that this is a favorable oscillatory state of ZP net for penetration and fertilization. In the case of chaotic like or stochastic like trajectories of molecules at the ZP surface net, the probability that one of many spermatozoa which are periodically "attacking" ZP to penetrate through is very low. In this case it is more likely that the incoming sperm cells will have impact with ZP molecules.

1.2. The basic assumptions of the oscillatory model of ZP

The mechanical model of discrete oscillatory spherical net of mZP was created by using discrete continuum method [29–31]. Dynamics of oscillatory discrete spherical net ZP model are described by a system of differential equations along component displacements in the radial w_{ij}, circular $u_{i,j}$, and meridian $v_{i,j}$ directions.

Chains in the meridian and circular directions are orthogonal. Crossed chains are forming the spherical net with same properties in the circular and meridian directions. Chains in the circular and meridian directions lie in the spherical concentric circles to the oocyte that we suppose is solid and elastic.

Chains are composed of the molecules of ZP glycoproteins as material particles of different masses interconnected with massless, in this case, linear elastic elements in a specific manner.

Each ZP protein molecule is coupled to the oocyte sphere boundary surface by elastic springs that can oscillate in radial direction.

Each of knot molecules has three degrees of freedom of motion, in the radial, circular, and meridian directions, while other molecules in mZP sphere surface model have two, in the circular and radial or in the meridian and radial directions.

1.2.1. Free oscillations

We consider that the system of ZP oscillatory net oscillates in a free regime after ovulation without presence of spermatozoa. If there is only an initial perturbation by the kinetic and/or potential energy given to oscillatory structures, only free vibration regimes of the vibrating discrete structure will appear. In this case material particles at the initial moment obtain the initial displacements, measured from their equilibrium positions, and initial velocities. Free oscillations can appear, if only one mass particle position is perturbed from its equilibrium position or if only one mass particle at its equilibrium position obtains initial velocity.

1.2.2. Forced vibrations

When one or more spermatozoa impact with the surface of ZP discrete spherical net, we assume that ZP oscillates in a forced regime at a single-frequency or a multiple frequency.

Goal of the current research is to assess if oscillations of mZP could be influenced by sperm impact angles.

Therefore, the resultant trajectories of knot molecules oscillating at multiple frequencies, under different external excitation conditions, under different impact angles of spermatozoids having an effective velocity have been analyzed.

A qualitative analysis of the influence of different sperm impact angles on the resultant oscillatory movements of knot molecules in the context of favorable angles for fertilization was performed.

2. The analysis of oscillatory behavior of knot molecules in mZP spherical net model through generalized Lussajous curves

For the analysis of generalized Lissajous curves of knot molecule trajectories of spherical surface net of mZP when four spermatozoids having an effective velocity have impacts at four neighboring knot molecules, we use the method of discrete continuum [29–31].

A periodic force acting simultaneously upon knot molecules is applied in the model. The force intensity varies depending upon the impact angle and velocity. A local impact with one knot will influence the displacements of molecules in two neighboring orthogonal chains, therefore the resulting displacements of the knot molecules will be influenced by the symmetric/asymmetric action of the force upon neighboring knot molecules in the two orthogonal chains.

The case corresponding to in vitro conditions has been modeled. The model does not include cumulus oophorus cells since this is an additional modeling challenge. At present there are no attempts to include in the mechanical model of sperm–oocyte interaction the cumulus oophorus cells.

We took only one small part of the oscillatory sphere surface net of mZP with the minimal number of molecules that periodically repeat in the chains (11 molecules in a chain) that still preserves molar ratio of the mZP glycoproteins ZP1: (ZP2–ZP3)= 1:5 (see Fig. 1C).

We focused on the knot mass dynamics because chemical changes in ZP1 molecules are very important for the fertilization process (Wasserman from [26,6,7]). In Fig. 1B and C the knot molecules ZP1 are presented in orange.

In order to carry out frequency analysis of knot mass oscillation trajectories in oscillatory spherical net model of mZP, we have to pass through several steps:

- Defining differential equation of the chains dynamics with the motion of 11 material particles;
- Making assumption as regards solutions and determining the system of homogenous algebraic equations concerning eigen amplitudes of the mass particles;
- Determination of the system determinants and characteristic functions and the characteristic or frequency equation of the system oscillatory behavior;
- Determination of the set of 11 eigen frequencies;
- Determination of cofactors which correspond to each of the 11 eigen frequencies and the corresponding eigen amplitudes which correspond to each of the 11 eigen frequencies;
- Determination of analytical expressions for each of the 11 mass particle displacements in the chain direction and the corresponding integral constants for the corresponding particular and defined initial conditions;
- Performing numerical multi-parameter analysis for certain initial conditions of the system dynamics.

We assume that rigidities (c_m) of the massless elastic elements, which interconnect the ZP molecules, are equal and calculated by

$$c_m = \frac{E\left(R^2 - r^2\right)\pi}{2R},\qquad(1)$$

where E is Young module of elasticity, R is radius of the mouse oocyte, r is radius of the oocyte minus approximate thickness of mZP. Data were taken from the paper by Sun et al. [6].

In particular, $E = 17.5$ kPa, $2R = 56.5$ μm-average diameter of the oocyte from [6], $\delta = 4.94$ μm-approximate thickness of the oocyte, and $c_m = 0.253$ N/m.

Molecular masses of the corresponding ZP glycoproteins were transformed into standard units.

Eigen circular frequencies $\omega_s, s = 1, 2, 3, ..., 11$, were calculated by formula: $\omega_s(x_s) = 10^6\sqrt{x_s}$, $s = 1, 2, 3, ..., 11$, where x_s is reduced non-dimensional value of the square eigen circular frequency, read from the graphic, 10^6 is factor of correction. We use the corrected factor for two reasons: to harmonize the measurement units and because ZP glycoprotein molecular masses in Matcad calculations are multiplied by 10^{12}.

For displacements' analysis of the system described in Fig. 1C, we used a system of ordinary differential equations consisting of three subsystems:

Subsystem of ordinary differential equation (2) describes free vibrations of the knot molecules in the radial direction:

$$m_{ij}\ddot{w}_{ij} = -c_{(w)ij}w_{ij} + F_{i,j}\sin\left(\Omega_{ij}t\right),\quad ij = 1,2;1,4;3,2;3,4,\qquad(2)$$

where m_{ij} are masses of the knot molecules in the cross-section of ith chain in the circular direction, $i = 1, 3$ and jth chain in the meridian direction $j = 2, 4$. These knot molecules are third/ninth in the corresponding circular, or meridian chain; $c_{(w)ij}$ is the rigidity of spring in radial direction, between the knot molecule and spherical surface of the oocyte; w_{ij} is the component displacement in the radial direction of a knot molecule of mass m_{ij} in an orthogonal cross section between ith chain in the circular and jth chain in the meridian direction;

$\ddot{w}_{ij}$ is the radial component of acceleration in direction of the knot molecule of mass m_{ij} in the orthogonal cross section between ith chain in the circular and jth chain in the meridian direction; $\left(-m_{ij}\ddot{w}_{ij}\right)$ is the radial component of inertial force of the knot molecule of mass m_{ij} in the orthogonal cross section between ith chain in the circular and jth chain in the meridian direction; $F_{i,j}$ is the amplitude of external excitation force applied in the radial direction of knot molecule of mass m_{ij}; Ω_{ij} is the circular frequency of external excitation force applied in the radial direction to the knot molecule of mass m_{ij} in the orthogonal cross section between ith chain in the circular and jth chain in the meridian direction.

Subsystem of ordinary differential equations describing free vibrations of molecules in the circular direction:

$$m_{ij}\ddot{u}_{ij} = +c_{(u)ij}\left(u_{i+1j} - u_{ij}\right) - c_{(u)i-1j}\left(u_{ij} - u_{i-1j}\right),\quad i = 1, 2, 3, ..., 11, j = 1, 3\qquad(3)$$

where m_{ij} are mass of molecules in jth circular chain $j = 1, 3$, and in ith order along circular chains containing 11 molecules, $i = 1, 2, 3, ..., 11$ (see model in Fig. 1C); u_{ij} is the circular component of displacement of molecule with mass m_{ij} in jth circular chain $j = 1, 3$, and in ith order along circular chains containing 11 molecules $i = 1, 2, 3, ..., 11$; $\ddot{u}_{ij}$ is the circular component of acceleration of molecule of mass m_{ij} in jth circular chain $j = 1, 3$, and in ith order along circular chains containing 11 molecules $i = 1, 2, 3, ..., 11$; $\left(-m_{ij}\ddot{u}_{ij}\right)$ is the circular component of the force of inertia of molecule of mass m_{ij} in jth circular chain $j = 1, 3$, and in ith order along circular chains containing 11 molecules $i = 1, 2, 3, ..., 11$; $c_{(u)ij}$ is the rigidity of spring between two mass particles $m_{i-1,j}$ and m_{ij} in circular chains; $\left(u_{i+1j} - u_{ij}\right)$ is the axial

deformation (extension or compression) of the spring of rigidity $c_{(w)ij}$ between two neighboring molecules $m_{i-1,j}$ and m_{ij} in the circular chains; and $\left(-c_{(w)ij}(u_{i+1,j} - u_{i,j})\right)$ is the conservative force of elasticity that appears in a spring during its axial deformation.

Subsystem of ordinary differential equations describing free vibrations of molecules in the meridian direction in meridian chains:

$$m_{ij}\ddot{v}_{ij} = +c_{(v)i,j}\left(v_{i,j+1} - v_{i,j}\right) - c_{(v)i,j-1}\left(v_{i,j} - v_{i,j-1}\right),\quad i = 2, 4, j = 1, 2, 3, ..., 11\qquad(4)$$

where m_{ij} are mass particle in ith meridian chain $i = 2, 4$ and in jth order along meridian chains containing 11 molecules, $j = 1, 2, 3, ..., 11$ (see model in Fig. 1C); v_{ij} is the meridian component of displacement of a molecule of mass m_{ij} in ith meridian chain $i = 2, 4$, and in jth order along meridian chains containing 11 molecules, $j = 1, 2, 3, ..., 11$; $\ddot{v}_{ij}$ is the meridian component of acceleration of molecule of mass m_{ij} in ith meridian chain $i = 2, 4$, and in jth order along meridian chains containing 11 molecules, $j = 1, 2, 3, ..., 11$; $\left(-m_{ij}\ddot{v}_{ij}\right)$ is the meridian component of force of inertia of molecule of mass m_{ij} in ith meridian chain $i = 2, 4$, and in jth order along meridian $j = 1, 2, 3, ..., 11$ containing 11 molecules; $c_{(u)ij}$ is the spring rigidity in meridian chains; $\left(v_{i,j+1} - v_{i,j}\right)$ is the spring dilatation/axial deformation (extension or compression) of a spring of rigidity $c_{(u)ij}$ between two neighboring molecules; $\left(-c_{(v)i,j}(v_{i,j+1} - v_{i,j})\right)$ is the conservative force which appears in the spring of rigidity $c_{(u)ij}$ between two mass particle $m_{i,j-1}$ and m_{ij} in meridian chains, as a result of the spring deformation (extension or compression).

Eqs. (2)–(4) were obtained from [22] and they correspond to Fig. 1C.

3. Impact of the four spermatozoa having an effective velocity

We analyzed a multiple-frequency oscillatory motions of knot molecules when each of the four sperm cells of an effective velocity simultaneously impact with different neighboring knot molecules (see Fig. 1C). By simulating *in vitro* conditions when an oocyte is acted upon by several spermatozoa [2], we considered a small segment of the ZP model (see Fig. 1C) when all available knot molecules are exposed to external periodic forces. A higher number of spermatozoa per one egg cell is biomechanically justified, i.e. mass of an egg cell is 10^7 times higher than the mass of an individual spermatozoid. Owing to this high difference between masses of the two cells, the egg cell in this system practically behaves as a highly inertial body. A spermatozoid which periodically acts on the surface of the oocyte cannot generate sufficient pressure ensuring its penetration through the ZP thickness. We consider that a simultaneous periodic action of a number of spermatozoa covering the whole surface of the egg cell could generate sufficient force which would, at certain point, weaken the ZP shell and enable penetration of a single spermatozoid. Also, within the oscillatory theory of fertilization, which is a part of this oscillatory model, we consider that the weak point is generated at the place where the resonance has appeared since, phenomenologically, it can raise the amplitude of molecular oscillations to a degree causing a break of the bond between them. Since the area and structure of ZP, as well as the surface of spermatozoid heads and their dynamical characteristics, are specific for the minimum number of spermatozoa required for fertilization, this minimum number of spermatozoa is species dependent.

Data for the mouse spermatozoa of effective velocity *Vhp* from [32] were taken to and represent average path velocity of hyper-activated sperm cells, $Vhp = 171.1$ μm/s. The hyper-activated sperm cells were considered as the sperm cells of effective

velocity. Hyper-activation of sperm cells is necessary for the capacitating process whereby sperm cells become competent to fertilize the oocyte [33]. According to the data for the mass of bull spermatozoa (1.82×10^{-14} kg or 1.82×10^{-11} g) [34], the approximated mass for a mouse spermatozoon was taken as 10^{-14} kg (10^{-11} g).

The velocity which spermatozoa transfer to the knot molecule at the moment of impact was calculated according to formula: $V = Vhp \times Msp/m_3$. Msp is the approximated mass of mouse spermatozoa; m_3 is mass of ZP1 glycoprotein-knot molecule.

When spermatozoa exerts influence on a plane that intersects the plane tangential to the sphere, and when direction of spermatozoa's movements forms an angle γ with the tangential plane, i.e. angle $\pi/2$ with radial plane, angle θ with meridian direction, i.e. angle $90 - \theta$ with circular direction, spermatozoa movement speed can be decomposed into three components: circular, meridian, and radial, according to the formulas:

$$V_{cir} = V \cos(\gamma) \sin(\theta), \tag{5}$$

$$V_{mer} = V \cos(\gamma) \cos(\theta), \tag{6}$$

$$V_{rad} = V \sin(\gamma). \tag{7}$$

Analytical expressions for the oscillatory movements of knot molecules in mZP spherical surface net model in the circular and meridian directions could be written as a superposition of 11 collinear asynchronous modes in the following forms:

$$u_3(t) = \sum_{s=1}^{11} K_{3s} C_s \cos(w_s t + \alpha_s), \tag{8}$$

$$v_3(t) = \sum_{s=1}^{11} K_{3s} D_s \cos(w_s t + \beta_s), \tag{9}$$

$$wr_3 = 10^6 \sqrt{\frac{c_m}{m3}}, \quad w_3(t) = \frac{V}{wr_3} \sin(\gamma) \sin(wr_3 t), \tag{10}$$

where $u_3(t)$ is the displacement in the circular direction, $v_3(t)$ is the displacement in the meridian direction, and wr_3 is the displacement in the radial direction of the third molecule (knot molecule in the sphere surface net model of mZP) in the considered chain (for details see Ref. [35]), w_s is the eigen circular frequencies, K_{3s} is the cofactor of system determinante defining the characteristic (frequency) equation of the system for the corresponding value of Sth circular frequency, C_s and D_s, as well as α_s and β_s, are integral constants, determined by the initial conditions for each impact velocity of the spermatozoa into the corresponding knot mass particle. There are 11-frequency equations.

Eleven zeros (roots) of the system characteristic function are 11 squares of the corresponding 11 eigen circular frequencies of the considered subsystem of the discrete spherical surface net model. All 11 material particles in the chain oscillate at these 11 circular frequencies. These frequencies are characteristic for the system and its structure and do not depend upon initial conditions. They depend only upon molecular masses and rigidity of the springs' elements in the subsystem.

The corresponding superposition of the trajectory motion for each knot molecule in the corresponding plane was done for the cases when each of the 4 spermatozoa acts upon one of the knot molecules. The calculation was done for different sperm impact angles.

As the chains in the spherical surface mZP model are orthogonal, the resultant displacements of the knot molecules in the circular $u(t)$ and meridian $v(t)$ directions are obtained by summing the effect of three sperm cells on the neighboring knot molecules.

The example of equations for displacement in the circular and meridian directions of the first knot molecule is presented by formulas:

$$u_1(t) = u_{3,N_1}(t) + u_{9,N_2}(t), \tag{11}$$

$$v_1(t) = v_{3,N_1}(t) + v_{9,N_4}(t), \tag{12}$$

where N_1–N_4 denotes position of the knot molecule in the corresponding chain in the part of the spherical net, indexes 3 and 9 denote order of molecules in the chain (see Fig. 1B). We introduced this notation so that different initial conditions could be applied to each knot molecule by using analytical solutions for the mass particle in the 11-mass particle model of the chain and to use the corresponding analogy and cyclic permutation of the order indices of the knot mass particles (sperm impact angle and sperm velocity). Expressions for the second, third, and fourth knot molecule are of the same form – summing the effect of the neighboring knot molecules. These formulas are generated from the model.

When one sperm cell has periodical repetitive impact on the first knot molecule, then it causes displacements of all molecules in the chain. We are interested in the resultant trajectory of the knot molecules (third and ninth in the chain) in the plane tangential to the sphere net. Displacements in the circular and meridian directions caused by a periodical impact of the sperm cell at the first knot molecule are calculated according to the formulas:

$$u_{3,N_1}(t) = V_1 \sum_{s=1}^{11} K_{3s} C_{1s} \cos(w_s t + \alpha_{1s}), \tag{13}$$

$$v_{3,N_1}(t) = V_1 \sum_{s=1}^{11} K_{3s} D_{1s} \cos(w_s t + \beta_{1s}), \tag{14}$$

$$u_{9,N_1}(t) = V_1 \sum_{s=1}^{11} K_{9s} C_{1s} \cos(w_s t + \alpha_{1s}), \tag{15}$$

$$v_{9,N_1}(t) = V_1 \sum_{s=1}^{11} K_{9s} D_{1_s} \cos(w_s t + \beta_{1s}). \tag{16}$$

These formulas are generated on the basis of the theory of oscillations [35], in particular, theory of oscillations of chain systems [36] (for details see Ref. [35]). Equations for displacements of the corresponding knot molecules caused by the second, third, and fourth sperm cell are similar to those of the first.

In Eqs. (13)–(16), V_1 is ratio between the sperm effective velocity (velocity of hyperactivated mouse sperm taken from [32]) and velocity from the previous experiments. Like in the previous experiments, we took the same value for the hyperactivated sperm velocity ($Vhp = 171.1$ μm/s), i. e. $V_1 = 1$.

For the considered case, we determined C_s and D_s from the initial conditions in the following form:

$$D_s = \frac{V}{L}|\Delta_s| \cos(\gamma) \sin(\theta), \tag{17}$$

$$C_s = \frac{V}{L}|\Delta_s| \cos(\gamma) \cos(\theta), \tag{18}$$

where expression L has the following form:

$$L = \sum_{s=1}^{11} (-1)^{11+s}(w_s K_{11,S}|\Delta g_s|), \tag{19}$$

w_s, $s = 1, 2, 3, ..., 11$ is the corresponding eigen circular frequency.

In the previous expressions, determinants $|\Delta g_s|$, $s = 1, 2, 3, ..., 11$, were determined for all 11 eigen circular frequencies.

For the first eigen circular frequency,

$$|\Delta g_1| = \det[a_{ij}], \quad a_{ij} = \omega_j K i_j, \qquad (20)$$

where $i = 1,2,3,\ldots,10$, $j = 2,3,4,\ldots,11$ (for details see [35]).

Determinants $|\Delta_s|$ were determined for all 11 eigen circular frequencies. For the first eigen circular frequency,

$$|\Delta_1| = \det[a_{ij}], a_{ij} = \omega_j K i_j, \qquad (21)$$

where $i = 1,2,4,5,\ldots,11$, $j = 2,3,4,\ldots,11$ (for details see [35]).

These determinants, determined the integral constants for the initial conditions when velocity is transferred to the third molecule in the equilibrium state and all other molecules did not have any velocity. In the previous expressions for displacements, and in matrices, w_s is the corresponding eigen circular frequency, α_s and β_s are the phase and integral constants, determined by initial conditions.

4. The results and discussion

In our numerical experiments we took for initial conditions that α_s and β_s had equal value of $\pi/2$. By using Math Cad and graphical method for presenting the characteristic function from the frequency equations of the system, we determine 11 zeros (roots) of the system characteristic function which correspond to the 11 squares of the corresponding 11 eigen circular frequencies.

By assuming that all sperm cells have the same effective velocity: $Vhp = 171.1$ μm/s, $V_1 = V_2 = V_3 = V_4$, and the same impact angle with respect to the knot molecules, $\gamma_1 = \gamma_2 = \gamma_3 = \gamma_4$, $\theta_1 = \theta_2 = \theta_3 = \theta_4$, we analyzed the resultant trajectory of motions of the knot molecules.

For the specific (particular) values of the sperm impact angles γ and θ with respect to the knot molecules ($\pi/12$, $\pi/6$, $\pi/4$, $\pi/3$, $\pi/2$ and $2/3\pi$), the resulting displacements of the knot molecules are obtained. We varied the value of impact angle: from the cases when angles γ and θ were having the same value equal to $\pi/12$, $\pi/6$, $\pi/4$, $\pi/3$, $\pi/2$, and $2\pi/3$ to the cases when angles γ and θ were not equal. Different combinations of the before mentioned values of angles were used.

The resultant displacements of the knot molecules are in the form of generalized Lissajous curves obtained by summing two orthogonal (circular and meridian) component vibrations at 11-frequencies.

Depending upon the form of the obtained generalized Lissajus curves, we made a series of conclusions useful for evaluation of dynamical state of the ZP multiple-frequency oscillations.

The different cases when angles γ and θ are equal are presented in Figs. 2–4.

Generalized Lissajous curves in Fig. 2B has chaotic-like form showing that the $\pi/2$ sperm impact angle is not suitable for fertilization. It is the most unfavorable impact angle, although the amplitudes of motions of the knot molecules are very low (see also Figs. 6A, 7B,
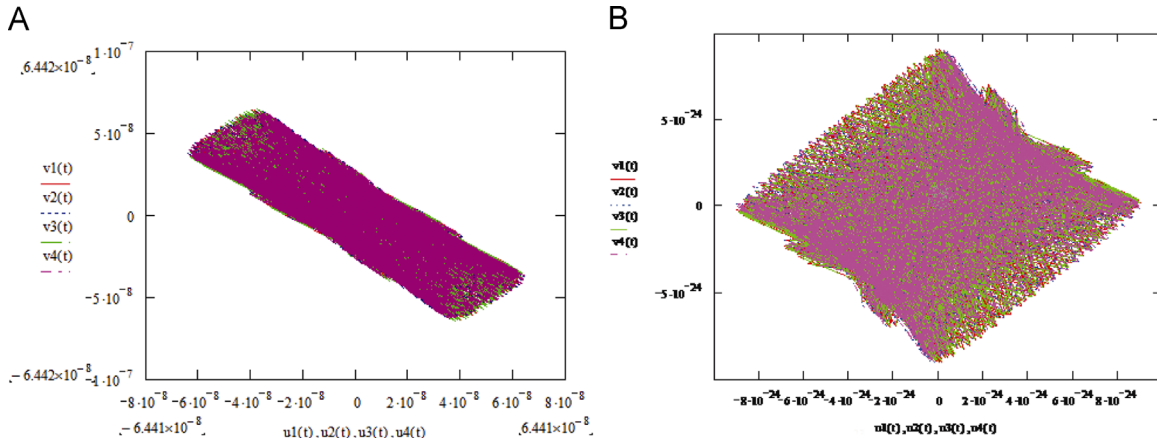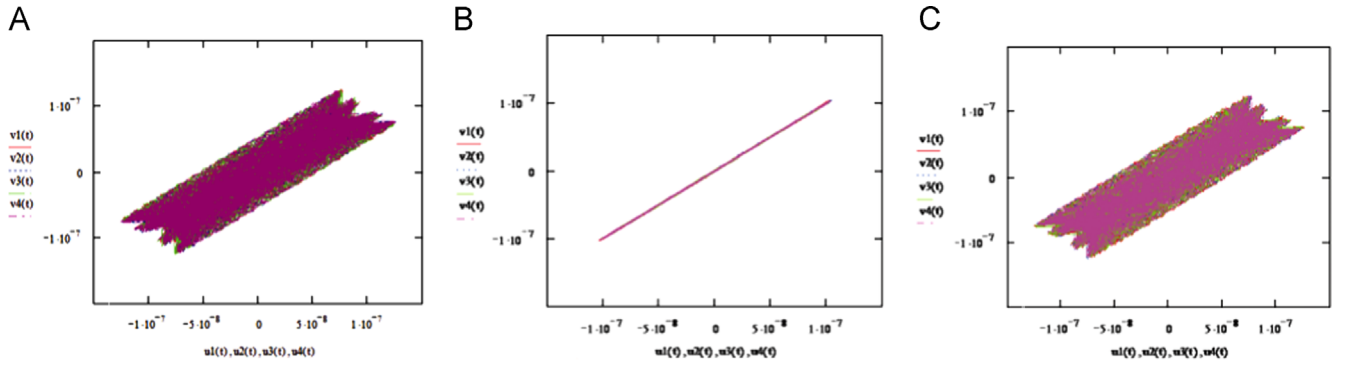

Fig. 2. Trajectories for all four knot mass particles when all four sperm cells have maximum velocities and impact angles γ and θ are equal – $\gamma_1 = \gamma_2 = \gamma_3 = \gamma_4 = \theta_1 = \theta_2 = \theta_3 = \theta_4$: (A) $2/3\pi$ and (B) $\pi/2$.
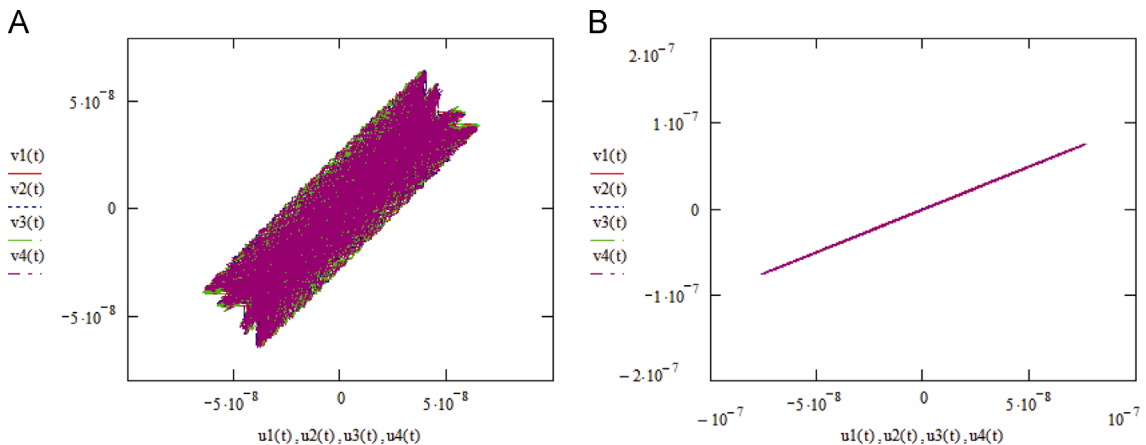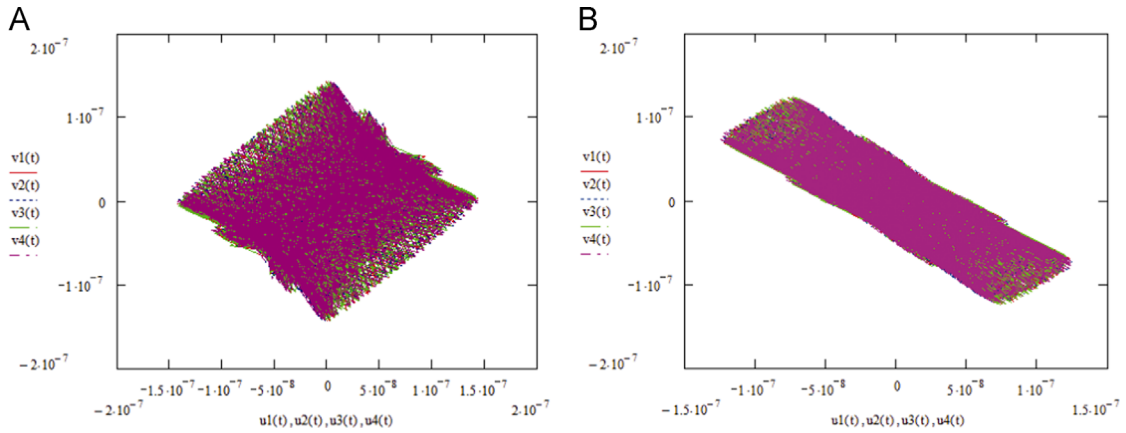

Fig. 3. Trajectories for all four knot mass particles when four sperm cells have maximum velocities and impact angles γ and θ are equal – $\gamma_1 = \gamma_2 = \gamma_3 = \gamma_4 = \theta_1 = \theta_2 = \theta_3 = \theta_4$ of: (A) $\pi/3$ and (B) $\pi/4$.
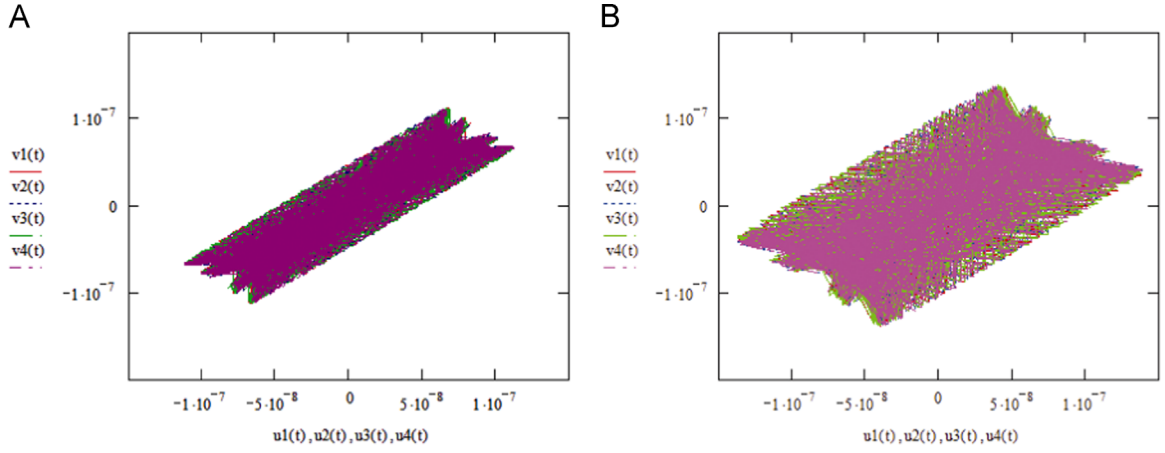
Fig. 4. Trajectories for all four knot mass particles when four sperm cells have maximum velocities and impact angles γ and θ are equal – $\gamma_1 = \gamma_2 = \gamma_3 = \gamma_4 = \theta_1 = \theta_2 = \theta_3 = \theta_4$ of: (A)$\pi/6$ and (B) $\pi/12$.

Fig. 5. Trajectories for all four knot mass particles when four sperm cells have maximum velocities and impact angles $\gamma_1 = \gamma_2 = \gamma_3 = \gamma_4 = \pi/12$ and $\theta, \theta_1 = \theta_2 = \theta_3 = \theta_4$ is equal to: (A) $\pi/6$, (B) $\pi/4$ and (C) $\pi/3$.

Fig. 6. Trajectories for all four knot mass particles when four sperm cells have maximum velocities and impact angles $\gamma_1 = \gamma_2 = \gamma_3 = \gamma_4 = \pi/12$ and θ $\theta_1 = \theta_2 = \theta_3 = \theta_4$ is equal to: (A) $\pi/2$ and (B) $2/3\pi$.

and 8A). Bedford [14] speculates that sperm impact angle of $\pi/2$ will probably provide holes in the ZP during its stretching during growth of the embryo. Angle $2\pi/3$, according to the form of generalized Lissajous curves, provides asynchronous dynamical state of the knot molecules (see Figs. 2A, 6B, 7C, and 8B, C).

In Fig. 3B is visible that all four knot molecules oscillate synchronously (angles γ and θ are equal to $\pi/4$).

For very small values of angles γ and $\theta < \pi/12$, Lissajous' curve has a chaotic-like appearance indicating that this combination of angles is not favorable for fertilization.

For the same initial conditions (at the initial moment, when equilibrium of the system of sphere surface net is exposed to the spermatozoa that transferred their kinetic energies to the knot molecule) at a given angle $\pi/12$ and with different values of angle θ, the resultant displacements of all four knot molecules are presented in Figs. 5 and 6.

When γ has value of $\pi/6$ and θ ($\theta_1 = \theta_2 = \theta_3 = \theta_4$) has values $\pi/4$ or $\pi/3$we obtained the same graphs as in Fig. 5B and C; when θ is $\pi/2$, $2\pi/3$ the resultant displacements of the knot molecules look like those presented in Fig. 6A and B respectively.
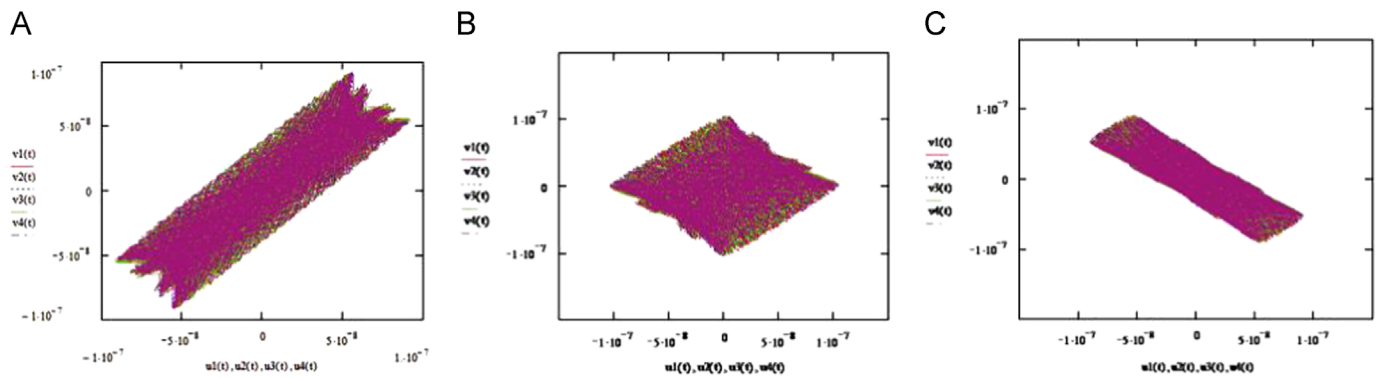
Fig. 7. Trajectories for all four knot mass particles when all four sperm cells have maximum velocities and impact angles $\gamma_1 = \gamma_2 = \gamma_3 = \gamma_4 = \pi/4$ and $\theta, \theta_1 = \theta_2 = \theta_3 = \theta_4$ is equal to: (A) $\pi/3$; (B) $\pi/2$ and (C) $2/3\pi$.
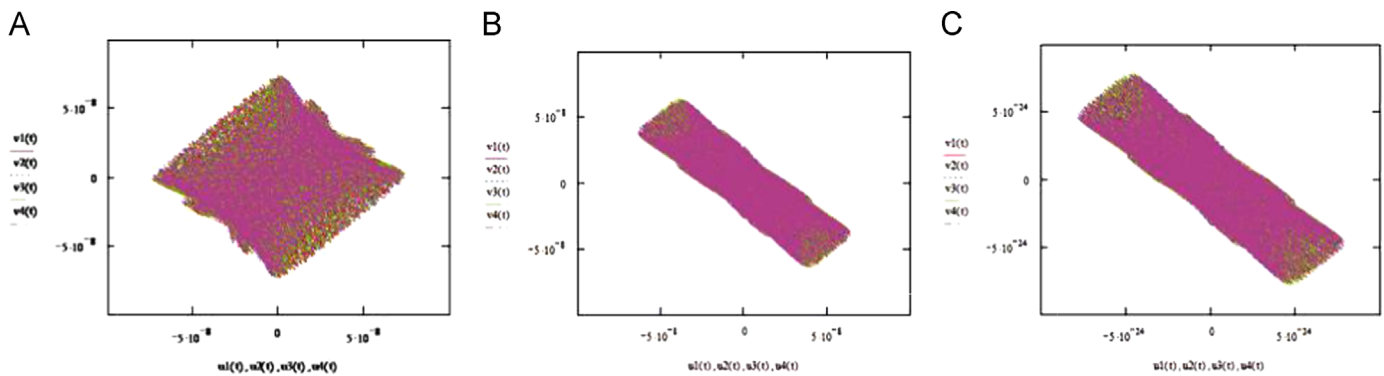
Fig. 8. Trajectories for all four knot mass particles when all four sperm cells have maximum velocities and impact angles: (A) $\gamma_1 = \gamma_2 = \gamma_3 = \gamma_4 = \pi/3$ and $\theta_1 = \theta_2 = \theta_3 = \theta_4 = 1/2\pi$. (B) $\gamma_1 = \gamma_2 = \gamma_3 = \gamma_4 = \pi/3$ and $\theta_1 = \theta_2 = \theta_3 = \theta_4 = 2/3\pi$. (C) $\gamma_1 = \gamma_2 = \gamma_3 = \gamma_4 = \pi/2$ and $\theta_1 = \theta_2 = \theta_3 = \theta_4 = 2/3\pi$.
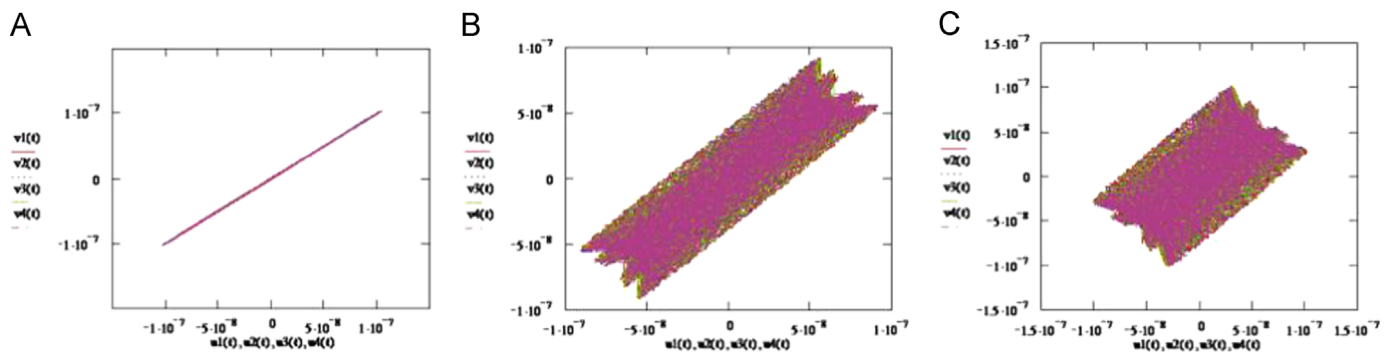
Fig. 9. Trajectories for all four knot mass particles when all four sperm cells have maximum velocities and impact angles: (A) $\gamma_1 = \gamma_2 = \gamma_3 = \gamma_4 = \pi/6$ and θ $\theta_1 = \theta_2 = \theta_3 = \theta_4 = \pi/4$ and $\gamma_1 = \gamma_2 = \gamma_3 = \gamma_4 = \pi/12$ and θ $\theta_1 = \theta_2 = \theta_3 = \theta_4 = \pi/4$. (B) $\gamma_1 = \gamma_2 = \gamma_3 = \gamma_4 = \pi/4$ and; $\theta_1 = \theta_2 = \theta_3 = \theta_4 = \pi/6$. (C) $\gamma_1 = \gamma_2 = \gamma_3 = \gamma_4 = \pi/4$ and $\theta_1 = \theta_2 = \theta_3 = \theta_4 = \pi/12$.

For sperm impact angle of $\pi/4$ and certain values of angle θ generalized Lissajous curves of the resultant displacements for all four knot molecules are presented in Fig. 7.

The resultant displacement for sperm impact angle $\pi/3$ and large values of angle θ are presented in Fig. 8A and B.

For combinations of angles γ and θ, $\pi/6$ and $\pi/4$ and $\pi/12$ and $\pi/4$ respectively, synchronization of all four knot molecules, each with 11-frequency vibrations, were obtained, (Fig. 9A) but for γ and θ $\pi/4$ and $\pi/6$ and $\pi/4$ and $\pi/12$ respectively, resultant motions for four knot molecules were in the form of chaotic like Lissajous curves (see Fig. 9B and C).

Favorable sperm impact angle γ of $\pi/12$ that we obtained in our numerical experiments in mZP spherical surface net model (see Figs. 5B and 9A) have a support by the results published in some papers in the area of reproductive biology and biophysical studies:

sperm surface remodeling necessary for fertilization [37,38], involving lipids and proteins that are organized into lateral regions of sperm head surface. These molecules enable a sperm cell to bind to the ZP [3].

The example when all sperm cells have different sperm impact angles with respect to knot molecules is presented in Fig. 10. In this case each knot molecule has different stochastic-like Lissajous curve, therefore this oscillatory state is not suitable for fertilization.

The best mechanical models of fertilization which appeared so far in the literature [17–19] confirmed that the speed of spermatozoa is more significant for the pressure a spermatozoid makes during its first contact with the surface of ZP than the density of spermatozoid heads or biochemical binding forces which exist between the surfaces of spermatozoids and ZP. These models
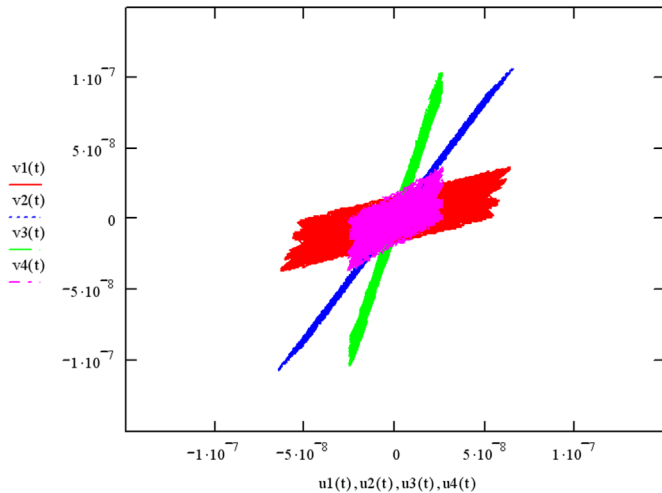
Fig. 10. Trajectories of all four knot mass particles when all four sperm cells have maximum velocities and different sperm impact angles: $\gamma_1 = \pi/3$ and $\theta_1 = \pi/6$, $\gamma_2 = \pi/4$ and $\theta_2 = \pi/6$, $\gamma_3 = \pi/4$ and $\theta_3 = \pi/2$, $\gamma_4 = \pi/2$ and $\theta_4 = \pi/4$.

consider only the influence of a single spermatozoid upon ZP surface.

The model of oscillatory spherical ZP net considers influence of a large number of spermatozoa (the situation usually existing in *in vitro* conditions and in majority of mammals also in *in vivo* conditions), which allows making the analyses of the influence of distribution of force and influence of the angle and speed upon oscillatory behavior of ZP.

Compared to the existing mechanical models, the model of oscillatory spherical ZP net differs in that the previous mechanical models did not take into account the impact angle of spermatozoa, not even as a potentially modifying factor for the force of impact a spermatozoid makes at ZP surface. The previous mechanical models make an *ad hoc* assumption that the impact angle is 90° and analyze the force generated by a spermatozoid starting from the assumption that the least contact surface will generate the highest pressure on ZP and that this highest pressure is required for spermatozoid penetration. However, the highest contact pressure will cause the highest resistance in ZP [39], since ZP exhibits viscoelastic properties and does not behave like an ideal elastic body [39]. Indeed, the exact mechanism of spermatozoid penetration through ZP is still unknown and it is not known whether the highest pressure made by spermatozoid corresponds to the most favorable mechanism for its penetration or it penetrates ZP following the line of "least resistance", i.e. it is easiest to penetrate at the point where ZP makes the least resistance [39].

There are articles where it is pointed that the transversal force generated by a spermatozoid is higher than the propulsive force [40,41] indicating that a sharp angle would be more favorable for the penetration. By using the mZP oscillatory spherical net model in our numerical experiments, we have come to the conclusion that sharp angles are more favorable, particularly $\pi/4$ and combinations $\pi/4$ and $\pi/12$ or $\pi/4$ and $\pi/6$. In addition to the findings in [40] and our own results, we consider that a lateral contact, i.e. sharp impact angle of spermatozoid collision, provides a larger contact surface between the spermatozoid and ZP which may facilitate receptor recognition between the two contact surfaces leading to a potentially easier penetration mediated predominantly by biochemical mechanisms.

It is possible to apply a wider range of speeds, but this, for the same angle, would change amplitudes of the movement of knot points – the moving trajectory remaining the same.

If a large number of spermatozoids effectuate periodic actions at ZP surface, there are countless combinations of angles and

speeds for both, individual and collective, actions upon the whole ZP system. There are combinations, not taken into account in this work, which could bring ZP to a state of excitation which is favorable for fertilization.

4.1. Limitations of the model

The main limitations of our model are related to the small number of elements in the model (four orthogonal chains, 11 molecules each), the model is linear, and chains in the model are orthogonal. This mechanical oscillatory model of ZP is based on the structural model of ZP, proposed by Wasserman in 1988 and modified later by Green in 1997 [26]. The essential difference is that the modified, Green's, model is a structural model whereas our's is an oscillatory model where ZP is represented by a spherical net surrounding oocyte. This net consists of the chains of ZP glukoproteins we assumed to be orthogonal and consisting of the glycoprotein's similarly distributed like in Wasserman's model, with the difference that the distribution of ZP2 and ZP3 is selected so that, even in the smallest unit, molar ratio of ZP molecules is preserved to be the same as the one existing in the ZP of mice. In reality, we do not know what the distance in microns between two knot molecules of ZP1 is.

According to the theory of oscillations, oscillatory behavior of a system is defined by the mass of the system, its elastic properties (in the present case stiffness of the springs), and characteristics of the external force, particularly frequency. Consequently, molar ratio between masses of ZP glucoproteins will be of influence upon oscillatory behavior of our model.

In the regime of forced oscillations, either dynamic absorption or resonance could arise. In this work, we intended to show phenomenologically what would be the oscillatory behavior of knot molecules in the regime of multiple frequency oscillations taking the smallest possible segment of the model of ZP oscillatory network where the molar ratio of the molecules is preserved. As a measure of the influence of spermatozoa on ZP, we used periodical force acting simultaneously upon knot molecules. A local action upon a single knot point will influence displacements of both neighboring molecules of the orthogonal chain.

By analyzing oscillatory behavior of a finite number of molecules in the mZP spherical net model (11), a finite number of eigen circular frequencies was obtained. In a real ZP there are numerous ZP molecules and thus numerous eigen circular frequencies. It is possible to use a larger number of molecules. As the number of molecules in the system increases, the corresponding mathematical calculations becomes progressively more complicated and additional programming is required, but qualitatively essentially different results would not be obtained. By including a larger number of molecules the model would become more cumbersome, the initial conditions would be changed, therefore there the results involving a higher number of frequencies and displacement coordinates would be obtained.

Non-linear properties of a real ZP and limitations of the analytical method of solving the corresponding system of non-linear differential equations require using numerical methods and approximations, or using oscillators with non-linear elastic and damping forces [42,43] in the modeling of oscillatory behavior of ZP. In a more complex model which includes non-linear bonds between molecules of the neighboring chains, the results related to synchronization of the movements of knot molecules inclusive of impact angle influence are similar [44].

Real ZP is a very complex oscillatory system and very selective as regards to spermatozoa penetration. This ZP selectiveness provides constant quantity of the genetic material in each generation.

5. The conclusions

By using the mechanical discrete spherical net model of mouse ZP, a qualitative analysis of oscillatory behavior of knot molecules in the model was done. From the frequency analysis of the knot molecules for forced vibrations caused by periodical impact of sperm cells under certain angle, we can conclude the following:

- Component displacements in the meridian and circular directions of knot molecules are in the form of multiple-frequency oscillations;
- Depending upon initial perturbation of the equilibrium state of material particles in the spherical net, component displacements of knot mass particles are in multiple-frequency oscillatory regimes, but with the number of frequencies is less or equal to the number of eigen frequencies of the system;
- The resulting trajectory of the component motions in the circular and meridian directions in the plane tangential to the sphere net of the observed knot molecules in the model are in the form of generalized Lissajous curves that could be in the form of strait line, periodical, non-periodical, stochastic-like or chaotic-like trajectories, as a results of summing two orthogonal multiple-frequency component vibrations. For obtaining a real space trajectory of a knot mass particle, the components in radial direction have to be added;
- Impact angles of the sperm cells' velocity directions have influence upon the resultant trajectories of motions of the knot molecules in the spherical net model of mZP;
- Impact angles of the sperm cells' velocity to the knot protein molecules are important for the resultant trajectories of motion and synchronism or asynchronism of multiple-frequency oscillatory motion of the knot protein molecules in the oscillatory spherical surface net model of mZP;
- We have identified the favorable and unfavorable sperm impact angles;
- Very small and very large impact angles are unfavorable;
- We confirmed that oblique angles are more favorable for fertilization and we predicted their values.

Synchronization of knot mass particle motions as results of summarizing of two orthogonal multi-frequency vibrations is not successful for spermatozoa that have impact to the knot mass particles in net, but this kinetic state could be an open pathway for some of next spermatozoa cell for successful passing through ZP and start fertilization;

The oscillatory spherical net model of mZP is suitable for modeling simultaneous influence of multiple sperm cells at the oocyte surface in *in vitro* conditions.

Combining the microscopy imaging techniques and mechanical model could be suitable for practical validation of the results of our numerical experiment: (i) are the sperm impact angles favorable for a successful fertilization predicted by the oscillatory model and (ii) are they identical or similar to the measured ones.

We believe that this oscillatory approach could contribute to better understanding of the fertilization process: how oocyte makes selection through its extra-cellular matrix? Does the receptor-mediated mechanism of recognition and fertilization have oscillatory phenomenon in its nature, like resonance between oscillatory regimes of ZP and "chosen" sperm cell as a necessary condition for fertilization?

Our analysis of the influence of sperm impact angle on parametric frequency analysis of the oscillatory behavior of knot molecules in mZP spherical net model is one step forward in understanding dynamical conditions and vibro-impacts in the processes of mammalian fertilization and polyspermy block.

Conflict of interest statement

None declared.

References

[1] N. Tipalski-Fišteš, Physiology of menstrual cycle and fertilization. In: Lj. Milašinović (Ed.), Physiology of Pregnancy, 1st ed. IP SKK Kosmos, Beograd, 2005, pp.41–59 (in Serbian).

[2] B. Nixon, R.J. Aitken, E.A. McLaughlina, New insights into the molecular mechanisms of sperm–egg interaction, Cell. Mol. Life Sci. 64 (14) (2007) 1805–1823.

[3] F.M. Flesch, M.B. Gadella, Dynamics of the mammalian sperm plasma membrane in the process of fertilization, Biochim. Biophys. Acta 1469 (2000) 197–235.

[4] E. Alegre, et al., Automatic classification of the acrosome status of boar spermatozoa using digital image processing and LVQ, Comput. Biol. Med. 38 (2008) 461–468.

[5] G.F. Clark, The molecular basis of mouse sperm–zona pellucida binding: a still unresolved issue in developmental biology, Reproduction 142 (2011) 377–381.

[6] Y. Sun, et al., Mechanical property characterization of mouse zona pellucida, IEEE Trans. Nanobiosci. 2 (2003) 279–286.

[7] Y. Murayama, et al., Mouse zona pellucida dynamically changes its elasticity during oocyte maturation, fertilization and early embryo development, Hum. Cell 19 (2006) 119–125.

[8] M. Papi, et al., Evidence of elastic to plastic transition in the zona pellucida of oocytes using atomic force spectroscopy, Appl. Phys. Lett. 94 (2009) 153902.

[9] M. Papi, et al., Mechanical properties of zona pellucida hardening, Eur. Biophys. J. 39 (2010) 987–992.

[10] M. Khalilian, et al., Estimating Young's modulus of zona pellucida by micropipette aspiration in combination with theoretical models of ovum, J. R. Soc. Interface 7 (2010) 687–694.

[11] M. Khalilian, et al., Alteration in the mechanical properties of human ovum zona pellucida following fertilization: experimental and analytical studies, Exp. Mech. 51 (2011) 175–182.

[12] A. Boccaccio, et al., Nanoscale characterization of the biomechanical hardening of bovine zona pellucid, J. R. Soc. Interface 9 (2012) 2871–2882.

[13] J.M. Bedford, Mammalian fertilization misread? Sperm penetration of the eutherian zona pellucida is unlikely to be a lytic event, Biol. Reprod. 59 (1998) 1275–1287.

[14] J.M. Bedford, Why do penetrating sperm create an oblique path in the zona pellucida? Reproduction 131 (2006) 23–25.

[15] D.A. Morales, E. Bengoetxea, P. Larrañaga, Selection of human embryos for transfer by Bayesian classifiers, Comput. Biol. Med. 38 (2008) 1177–1186.

[16] G. Corani, et al., A Bayesian network model for predicting pregnancy after in vitro fertilization, Comput. Biol. Med. 43 (2013) 1783–1792.

[17] A. Gefen, The relationship between sperm velocity and pressures applied to the zona pellucida during early sperm–oocyte penetration, J. Biomech. Eng. 132 (2010) 124501–124501-4.

[18] P. Kozlovsky, A. Gefen, The relative contributions of propulsive forces and receptor–ligand binding forces during early contact between spermatozoa and zona pellucida of oocytes, J. Theor. Biol. 294 (2012) 139–143.

[19] P. Kozlovsky, A. Gefen, Sperm penetration to the zona pellucida of an oocyte: a computational model incorporating acrosome reaction, Comput. Methods Biomech. Biomed. Eng. 16 (10) (2013) 7.

[20] A. Nir, The fertilization dance: a mechanical view of the egg rotation during the initial spermatozoa–ovum interaction, J. Theor. Biol. 214 (2002) 171–179.

[21] A. Hedrih, M. Ugrcic, Vibration properties characterization of mouse embryo during microinjection, Theor. Appl. Mech. 40 (S1) (2012) 189–202. http://dx.doi.org/10.2298/TAM12S1189H.

[22] A. Hedrih, Modeling oscillations of zona pelucida before and after fertilization, Young Scientist Prize Paper, Awarded at the 7th European Nonlinear Dynamics Conference held in Rome, Italy, July 2011, Euromech Newsletter 40, December,

European Mechanics Society, 40, 2011, pp. 6–14, ⟨http://www.euromech.org/prizes/presentations⟩; ⟨http://www.mi.sanu.ac.rs/projects/NL40-Euromech.pdf⟩.

[23] A. Hedrih, K. (Stevanovic) Hedrih, B. Bugarski, Oscillatory spherical net model of mouse zona pellucida, J. Appl. Math. Bioinform. 4 (2013) 225–268.

[24] A. Hedrih, M. Lazarevic, A. Mitrovic-Jovanovic, Parametric frequency analysis of oscillatory behaviour of mouse zona pellucida spherical net model: case successful and unsuccessful fertilization, Proc. Appl. Math. Mech. 13 (2013) 53–54.

[25] A. Hedrih, Transition in oscillatory behavior in mouse oocyte and mouse embryo trough oscillatory spherical net model of mouse Zona Pellucida, in: J. Awrejcewicz (Ed.), Applied Non-Linear Dynamical Systems, Springer Proceedings in Mathematics & Statistics, 93, Springer International Publishing, Switzerland, 2014, pp. 295–303. http://dx.doi.org/10.1007/978-3-319-08266-0__21.

[26] D. Green, Three-dimensional structure of the zona pellucida, Rev. Reprod. 2 (1997) 147–156.

[27] G. Familiari, et al., Three-dimensional structure of the zona pellucida at ovulation, Microsc. Res. Tech. 69 (2006) 415–426.

[28] G. Vanroose, et al., Structural aspects of the zona pellucida of in vitro-produced bovine embryos: a scanning electron and confocal laser scanning microscopic study, Biol. Reprod. 62 (2000) 463–469.

[29] A. Hedrih, Frequency Analysis of Knot Mass Particles in Oscillatory Spherical Net Model of Mouse Zona Pellucida Lecture Session, Short Paper, Abstract Book of 23rd International Congress of Theoretical and Applied Mechanics (IUTAM ICTAM Beijing) 19–24 August 2012, Beijing, China, SM01-049 Biomechanics and Biomaterials, 209 pp., ISBN 978-988-16022-3-7.

[30] K. Hedrih (Stevanovic), Discrete continuum method, in: Computational Mechanics, WCCM VI in Conjunction with APCOM 04, September 5–10, 2004, Beijing, China, Tsinghua University Press & Springer-Verlag, Beijing, pp. 1–11 (CD, International Association for Computational Mechanics (IACAM), www.iacm.info).

[31] K. Hedrih (Stevanovic), Modes of the homogeneous chain dynamics, Signal Process. 86 (2006) 2678–2702.

[32] S.G. Goodson, et al., Classification of mouse sperm motility patterns using an automated multiclass support vector machines model, Biol. Reprod. 84 (2011) 1207–1215.

[33] M.P. Curtis, et al., Modelling atethered mammalian sperm cell undergoing hyperactivation, J. Theor. Biol. 294 (2012) 139–143.

[34] G.F. Bahr, E. Zeitler, Study of bull spermatozoa. Quantitative electron microscopy, J. Cell Biol. 21 (1964) 175–189.

[35] P.D. Rašković, Theoy of Elastity, Naučna knjiga, Beograd, 1985 (in Serbian).

[36] K.R. (Stevanović) Hedrih, A.N. Hedrih, Phenomenological mapping and dynamical absorptions in chain systems with multiple degrees of freedom. J. Vib. Control (online first version of record – March 19, 2014) 10.1177/1077546314525984.

[37] M. Ikawa, N. Inoue, M. Okabe, Mechanisms of sperm–egg interactions emerging from gene-manipulated animals, Int. J. Dev. Biol. 52 (2008) 657–664.

[38] B.M. Gadella, Sperm membrane physiology and relevance for fertilization, Anim. Reprod. Sci. 107 (2008) 229–236.

[39] M. Papi, et al., Viscous forces are predominant in the zona pellucida mechanical resistance, Appl. Phys. Lett. 102 (2013) 043703. http://dx.doi.org/10.1063/1.4789503.

[40] S. Ishijima, Dynamics of flagellar force generated by a hyperactivated spermatozoon, Reproduction 142 (2011) 409–415.

[41] W.W. Hsiao, et al., Motility measurement of a mouse sperm by atomic force microscopy, Anal. Sci. 29 (2013) 3–8.

[42] L. Cveticanin, Oscillators with nonlinear elastic and damping forces, Comput. Math. Appl. 62 (2011) 1745–1757.

[43] L. Cveticanin, Forced pure nonlinear symmetrical oscillators, Math. Comput. Model. 55 (2012) 1580–1593.

[44] J. Simonovic, A. Hedrih, Synchronisation in oscillatory behaviour of embryo's ZP molecules in context of polyspermy block, in: Electronic USB Proceedings of 8th European Nonlinear Dynamics Conference (ENOC 2014), Nonlinear Dynamics in Biological Systems, July 6–11, 2014, Vienna, Austria, MS13-1.